FACULTY OF SCIENCE
UNIVERSITY OF COPENHAGEN

Master Thesis

Jian Wu – xcb479@alumni.ku.dk

Deep Contact

Accelerating Rigid Simulation with Convolutional Networks

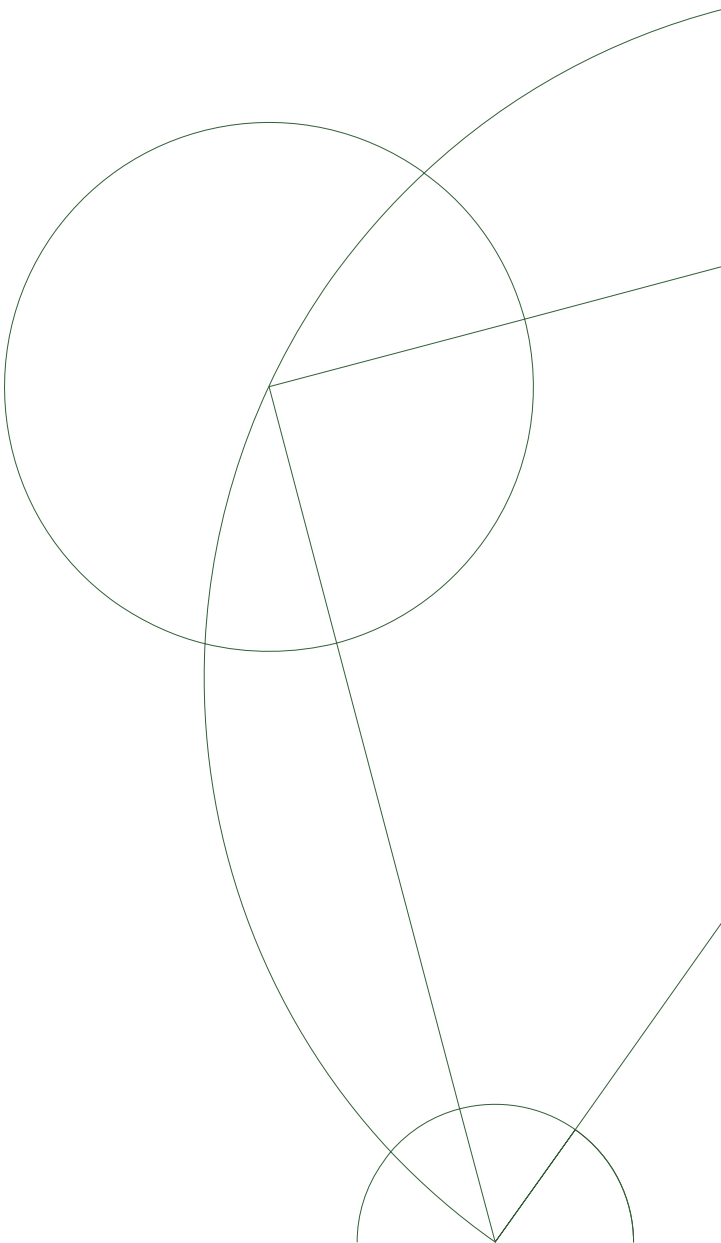

Supervisor: Kenny Erleben

August 6th 2018

Abstract

This is a master theis from

Contents

List of Figures

List of Tables

Chapter 1

Introdustion

1.1 Motivation

Movies studies have been pushing facial and character animation to a level where machine learning can automize a large part of this work in a production pipeline. Research community is exploring machine learning for gait control too and quite successfully or for upscaling of liquid simulation[1].

However, for rigid body problems it is not quite clear how to approach the technicalities in applying deep learning. Some work have been done in terms of inverse simulations or pilings to control rigid bodies to perform a given artistic 'target'. These thechniques are more in spirit of inverse problems that maps initial conditions to a well defined outcome(number of bounces or which face up on a cude) or level of detail idea replacing interiors of piles with stracks of cylinders pf decreasing radius to make an overall apparent pile have a given angle of of repose.

1.2 Thesis Overview

This thesis explore the application of convolutional neural networks in Computer Simulation.

Chapter 2

Rigid Body Dynamics Simulation

This chapter mainly introduces rigid body simulation to help you understand how computer simulate rigid dynamics based on traditional newton-euler equations. For more details, some contact forces solvers are decribed in this chapter. Afterwards, we will use one of solver to run some simulation and get the image data for the next step, grids-transfer. All the discussion about rigid simulation and contacts solver are based on 2-D view.

2.1 Rigid dynamics Simulation

2.1.1 Simulation Basics

Simulating the motion of a rigid body is almost the same as simulating the motion of a particle, so I will start with partcle simulation. For particle simulation, we let function $x(t)$ describe the particle's location in world space at time t. Then we use $v(t) = \frac{\mathrm{d}}{\mathrm{d}(t)}x(t)$ to denote the velocity of the particle at time t. So, the state of a particle at a time t is the particle's position and velocity. We generalize this concept by defining a state vector $\mathbf{Y}(t)$ for a system: for a single particle,

$$\mathbf{Y}(t) = \begin{pmatrix} x_1(t) \\ v_1(t) \end{pmatrix} \tag{2.1}$$

For a system with n particles, we enlarge $\mathbf{Y}(t)$ to be

$$\mathbf{Y}(t) = \begin{pmatrix} x_1(t) \\ v_1(t) \\ ... \\ x_n(t) \\ v_n(t) \end{pmatrix} \tag{2.2}$$

However, to simulate the motion of particles actually, we need to know one more thing – the forces. $F(t)$ is defined as the force acting on the particle. If the mass of the particle is m, then the changes of $\mathbf{Y}(t)$ will be given by

$$\frac{\mathrm{d}}{\mathrm{d}(t)}\mathbf{Y}(t) = \frac{\mathrm{d}}{\mathrm{d}(t)} \begin{pmatrix} x(t) \\ v(t) \end{pmatrix} = \begin{pmatrix} v(t) \\ F(t)/m \end{pmatrix} \tag{2.3}$$

2.1.2 Rigid Body Concepts

Unlike a particle, a rigid body occupies a volume of space and has a particular shape. Rigid bodies are more complicated, beside translating them, we can rotate them as well. To locate a rigid body, we use $x(t)$ to denote their translation and a rotation matrix $R(t)$ to describe their rotation.

2.1.3 Rigid Body Equations of Motions

Finally, we can covert all concepts we need to define the state $\mathbf{Y}(t)$ for a rigid body.

$$\mathbf{Y}(t) = \begin{pmatrix} x(t) \\ R(t) \\ P(t) \\ L(t) \end{pmatrix} \tag{2.4}$$

Like what is epressed in $\mathbf{Y}(t)$, the state of a rigid body is mainly consist by its position and orientation (describing spatial information), and its linear and angualr momentum(describe velocity information). Since mass M and bodyspace inertia tensor I_{body} are constants, we can the auxiliary quantities $I(t)$, $\omega(t)$ at any given time.

$$v(t) = \frac{P(t)}{M} \quad I(t) = R(t)I_{body}R(t)^T \quad \omega(t) = I(t)^{-1}L(t) \tag{2.5}$$

The derivative $\frac{\mathrm{d}}{\mathrm{d}t}\mathbf{Y}(t)$ is

$$\frac{\mathrm{d}}{\mathrm{d}t}\mathbf{Y}(t) = \frac{\mathrm{d}}{\mathrm{d}t}\begin{pmatrix} x(t) \\ R(t) \\ Mv(t) \\ L(t) \end{pmatrix} = \frac{\mathrm{d}}{\mathrm{d}t}\begin{pmatrix} v(t) \\ \omega(t) * R(t) \\ F(t) \\ \tau(t) \end{pmatrix} \tag{2.6}$$

Then, we can conclude the simulation algorithm
Data: this text
Result: how to write algorithm with LaTeX2e
initialization;
while *running the simulation world* **do**
    read current;
    if *understand* **then**
        go to next section;
        current section becomes this one;
    else
        go back to the beginning of current section;
    end
end

Algorithm 1: How to write algorithms

2.1.4 Twist/Wrench

We will now introduce vectors called twists, which describe velocities, and wrenches, which describe forces, and explain how these objects transform from one coordinate frame to another one.

Twist

Wrench

A wrench is a vector that expresses force and torque acting on a body. A wrench can be defined by

$$\mathbf{f} = \begin{pmatrix} \tau \\ f \end{pmatrix}$$

A wrench contains an angular component τ and a linear component f, which are applied at the origin of the coordinate frame they are specified in.

2.2 Constrained Dynamics

Most interesting simulations of rigid bodies involve some kind of constraints. Usually we want to model systems of bodies that are interacting in some way. Some bodies may be in contact with each other, or attached together by some types of joint. Since this report mainly research contact forces, we

2.2.1 Expressing Constraints as Equations

We express constraints mathematically as algebraic matrix equations with position, velocity, or acceleration vectors as the unknowns. In general, the configuration space of a set of n rigid bodies has dimension 6n. Adding constraint equations restricts the position (or velocity, or acceleration) to a subspace of smaller dimension.

The constraints discussed in this thesis will all be holonomic constraints, which means the constraint on the velocity can be found by taking the derivative of a position constraint. Constraints that do not fit this description are called nonholonomic. An example of a nonholonomic constraint is a ball rolling on a table without slipping. The position of the ball has five degrees of freedom, so there is only one degree of constraint (only the height is constrained). Taking the derivative of the position constraint would only give a velocity constraint of degree one. Additional constraints on the velocity are needed to prevent the ball from slipping.

We will describe position constraints with a constraint function $g(\mathbf{p})$, which is a function from the space of possible positions of the rigid bodies, to R , where

2.2.2 contact Constraints

2.2.3

Chapter 3

Partcle-grid-particle

The basic method for generating training data which is more accessible to learning is that we will map a discrete element method(DEM) into a continuum setting use techniques from smooth particle hydrodynamics. Given a set of bodies δ and a set of contacts between these bodies C.

3.1 Grid-Based method

Traditional rigid motion simulation mainly use particle-based method. However, if we want to replace traditional contact solver with deep learning model, it is hard for cnn model to recognize the original image and do learning. Grid-based methos is a good to transfer original image to a grid-cells and then use

3.2 Smoothed Particle Hydrodynamics

Smoothed particle hydrodynamics (SPH) was invented to simulate nonaxisymmetric phenoma in astrophysis initially. The principal

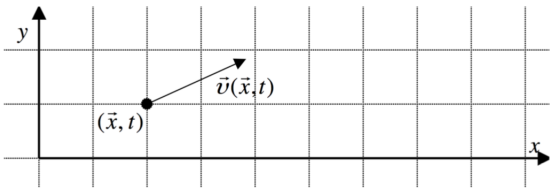

Figure 3.1: Grid description, $retrievedfromMIT$(2011)

idea of SPH is to treat hydrodynamics in a completely mesh-free fashion, in terms of a set of sampling particles. It turns out that the particle presentation of SPH has excellent conservation properties. Energy, linear momentum, angular momentum, mass and velocity.

3.2.1 Fundamentals

At the heart of SPH is a kernel interpolation method which allows any function to be expressed in terms of its values at a set of disordered points - the particles[2]. For ant field $A(\mathbf{r})$, a smoothed interpolated version $A_I(\mathbf{r})$ can be defined by a kernel $W(\mathbf{r}, h)$,

$$A_I(\mathbf{r}) = \int A(\mathbf{r}')W(\|\mathbf{r} - \mathbf{r}'\|, h)\,\mathrm{d}\mathbf{r}' \tag{3.1}$$

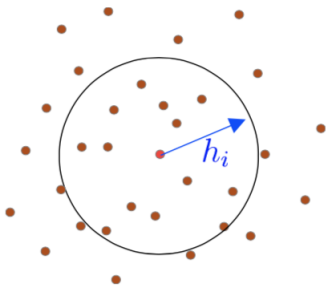

Figure 3.2: Visilaztion of SPH

where the integration is over the entire space, and W is an interpolating kernel with

$$\int W(\|\mathbf{r} - \mathbf{r}'\|, h)\,\mathrm{d}\mathbf{r}' = 1 \tag{3.2}$$

and

$$\lim_{h\to 0} W(\|\mathbf{r} - \mathbf{r}'\|, h)\,\mathrm{d}\mathbf{r}' = \delta(\|\mathbf{r} - \mathbf{r}'\|) \tag{3.3}$$

Normally, we want the kenel to be Non-negative and rotational invariant.

$$W(\|\mathbf{x}_i - \mathrm{x}_j\|, h) = W(\|\mathrm{x}_j - \mathrm{x}_i\|, h) \tag{3.4}$$

$$W(\|\mathbf{r} - \mathbf{r}'\|, h) \geq 0 \tag{3.5}$$

For numerical work, we can use midpoint rule,

$$A_I(\mathbf{x}) \approx A_S(\mathbf{x}) = \sum_i A(\mathbf{x}_i) W(\|\mathbf{x}_i - \mathbf{x}\|, h) \Delta V_i \tag{3.6}$$

Since $V_i = m_i/\rho_i$

$$A_S(\mathbf{x}) = \sum_i \frac{m_i}{\rho_i} A(\mathbf{x}_i) W(\|\mathbf{x}_i - \mathbf{x}\|, h) \tag{3.7}$$

The default, gradient and Laplacian of A are:

$$\begin{aligned} \nabla A_S(\mathbf{x}) &= \sum_i \frac{m_i}{\rho_i} A(\mathbf{x}_i) \nabla W(\|\mathbf{x}_i - \mathbf{x}\|, h) \\ \nabla^2 A_S(\mathbf{x}) &= \sum_i \frac{m_i}{\rho_i} A(\mathbf{x}_i) \nabla^2 W(\|\mathbf{x}_i - \mathbf{x}\|, h) \end{aligned} \tag{3.8}$$

3.2.2 Kernels

Smoothing kernels functions are one of the most important points in SPH. Stability, accurancy and speed of the whole method depends on these fuctions. Different kernels are being used for different purposes. One possibilyty for W is a Gaussian. However, most current SPH implementations are based on kernels with finite support. We mainly introduce gaussian, poly6 and spicky kernel here. And compare the different kernels and their property.

Poly6

The kernel is also known as the 6th degree polynomial kernel.

$$W_{poly6}(\mathbf{r}, h) = \frac{315}{64\pi h^9} \begin{cases} (h^2 - \|\mathbf{r}\|^2)^3 & 0 \le \|\mathbf{r}\| \le h \\ 0 & \text{Otherwise} \end{cases} \tag{3.9}$$

Then, the gradient of this kernel function can be

$$\nabla W_{poly6}(\mathbf{r}, h) = -\frac{945}{32\pi h^9} \begin{cases} \mathbf{r}(h^2 - \|\mathbf{r}\|^2)^2 & 0 \le \|\mathbf{r}\| \le h \\ 0 & \text{Otherwise} \end{cases} \tag{3.10}$$

The laplacian of this kenel can be expressed by,

$$\nabla^2 W_{poly6}(\mathbf{r}, h) = -\frac{945}{16\pi h^9} \begin{cases} (h^2 - \|\mathbf{r}\|^2)(3h^2 - 7\|\mathbf{r}\|^2) & 0 \le \|\mathbf{r}\| \le h \\ 0 & \text{Otherwise} \end{cases} \tag{3.11}$$

As Müller stated[3], if the kernel is used for the computation of pressure forces, particles tend to build cluster under high pressure because 'as particles get very close to each other, the repulsive force vanishes because the gradient of the kerbek approaches zero to the center.', which we can see in Figure 3.4. Another kernel, spiky kernel, is proposed by Desbrum and Gascuel[4] to solve this problem.

Spicky

The kernel proposed by Desbrum and Gascuel[4]

$$W_{spiky}(\mathbf{r}, h) = \frac{15}{\pi h^6} \begin{cases} (h - \|\mathbf{r}\|)^3 & 0 \leq \|\mathbf{r}\| \leq h \\ 0 & \text{Otherwise} \end{cases} \tag{3.12}$$

Then, the gradient of spiky kernel can be described by,

$$\nabla W_{spiky}(\mathbf{r}, h) = -\frac{45\mathbf{r}}{\pi h^6 \|\mathbf{r}\|} \begin{cases} (h - \|\mathbf{r}\|)^2 & 0 \leq \|\mathbf{r}\| \leq h \\ 0 & \text{Otherwise} \end{cases} \tag{3.13}$$

The laplacian of spiky can be expressed by,

$$\nabla^2 W_{spiky}(\mathbf{r}, h) = \frac{90}{\pi h^6} \begin{cases} h - \|\mathbf{r}\| & 0 \leq \|\mathbf{r}\| \leq h \\ 0 & \text{Otherwise} \end{cases} \tag{3.14}$$

3.2.3 Grid size and smoothing length

The grid should be also fine enough to capture the variation in our simulation. In our case, it is reasonable to have a grid fine enough such that no two contact points are mapped into the same cell.

Smoothing length, h, is one of the most important parameters that affects the whole SPH method by changing the kernel value results abd neighbor searching results. Too small or too big values might cause lose essencail information in the simulation.

3.2.4 Neignbor Search

Neighbor search is one of the most crucial procedures in SPH method considersing all interpolation equations, $A(\mathbf{r})$, needs the neighbor list for every particle (refer to equation 3.8). A naive neighbor searching approach would end up with a complexity of $o(n^2)$. The complexity

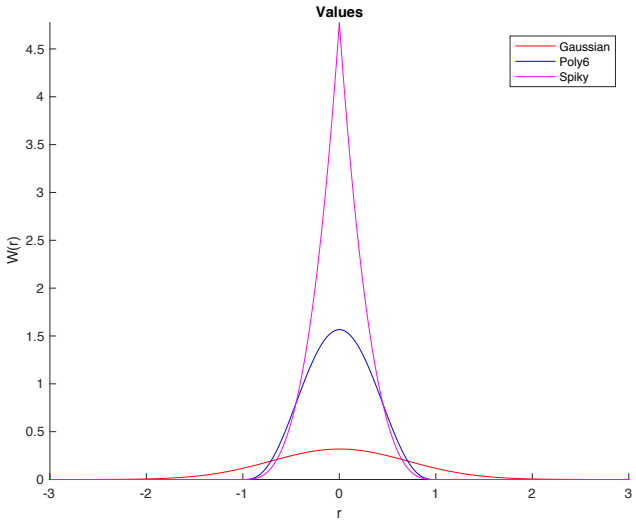

Figure 3.3: Comparation of different kernels, we set smoothing length $h = 1$ here.

is not good enough since it is impossoble to reach any interactive speed when the particle count increses. With an efficient nearest neighbor searching(NNS) algorithm, it is possible to have a significant performance increase since it is the most time consuming procedure in SPH computation. In order to decrease the complexity, we choose to use $k - d$ tree data structure to store the particla spatial information and then do the nearest neighbor searching.

Hierarchical Tree

Using an adaptive hierarchy tree search is proposed by Paiva[5] to find particle neighbors. Since the simulation takes place in two dimensions, $k - d$ tree data structure was used in this approach.

An octree structure has been adapted from Macey (b) Octree Demo. The hierarchy tree is formed with a pre-defined height. The simulation box is divided recursively into eight pieces, nodes. The nodes at height $= 1$ are called leaves. Each node has a surrounding box for particle query which is used to check if the particle is inside the node. Each parent node, contains the elements that are divided

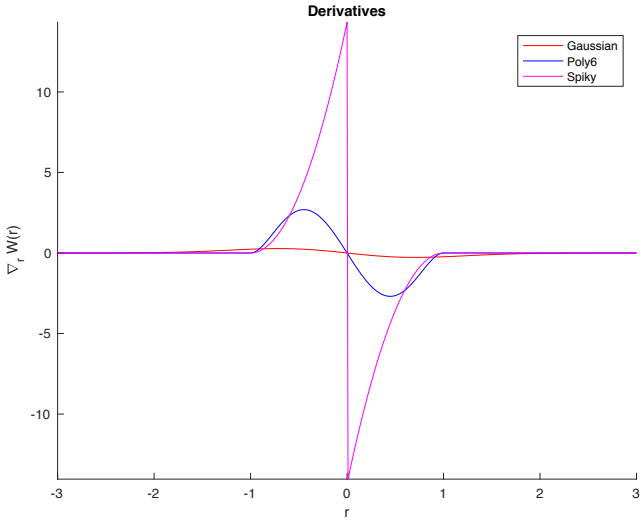

Figure 3.4: Comparation of gradient of different kernels, we set $h = 1$ here.

through its children. The particle is being checked at each level of the tree if it's intersecting the node. If it does, descend one level down in that node. After reaching to leaves, bottom level, particle has been checked if its within the search distance, h. If the particle is in the range, add it to the neighbor list. Neighbor searching is done when the whole tree has been traversed. The search distance set to be smoothing length in this implementation.

The complexity of this tree search method is $O(nlog(n))$, n being the number of particles. The performance of this algorithm is worse than Spatial Hashing method. In addition, the results obtained using this NNS algorithm wasn't accurate and stable for this implementation. Therefore as mentioned above, Spatial Hashing method was preferred.

3.3 Grid to particle

After getting the grid image for simulation state in time t, we will use the grid cells as input and renew the grid image based on trained

model. Once the grid image in $t + \Delta t$ have been renewed, the next step is to transfer the grid to particles which will instore all information including velocity,

3.3.1 Bilinear interpolation

We applied bilinear interpolation in our case, since we did mainly research on a rectilinear $2 - D$ grid. The key idea is to perform lin-

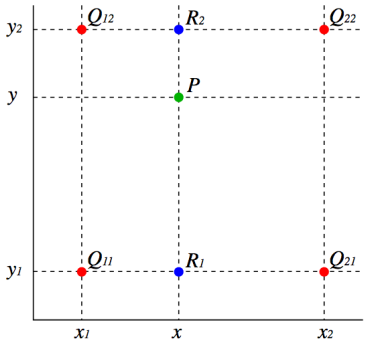

Figure 3.5: The figure shows visiualization of bilinear interpolation. The four red dots show the data points and the green dot is the point at which we want to interpolate.

ear interpolation first in one direction, and then again in the other direction. Although each step is linear in the sampled values and in the position, the interpolation as a whole is not linear but rather quadratic in the sample location.

As shown in Figure 3.5, We have known $Q_{a,b} = (x_a, y_b)$ and $a \in \{1, 2\} \quad b \in \{1, 2\}$. Then, we can firstly do linear interpolation in the x-direction. This yields

$$\begin{aligned} f(x, y_1) &\approx \frac{x_2 - x}{x_2 - x_1} f(Q_{11}) + \frac{x - x_1}{x_2 - x_1} f(Q_{21}), \\ f(x, y_2) &\approx \frac{x_2 - x}{x_2 - x_1} f(Q_{12}) + \frac{x - x_1}{x_2 - x_1} f(Q_{22}). \end{aligned} \tag{3.15}$$

After getting the two values in $x-$direction $f(x, y_1)$ and $f(x, y_2)$, we can use these values to do interpolation in $y-$ direction.

$$f(x, y) \approx \frac{y_2 - y}{y_2 - y_1} f(x, y_1) + \frac{y - y_1}{y_2 - y_1} f(x, y_2) \tag{3.16}$$

Combine $f(x, y_1)$ and $f(x, y_2)$ defined in equation 3.15, we can get,

$$\begin{aligned} f(x,y) &\approx \frac{y_2 - y}{y_2 - y_1}\left(\frac{x_2 - x}{x_2 - x_1} f(Q_{11}) + \frac{x - x_1}{x_2 - x_1} f(Q_{21})\right) \\ &\quad + \frac{y - y_1}{y_2 - y_1}\left(\frac{x_2 - x}{x_2 - x_1} f(Q_{12}) + \frac{x - x_1}{x_2 - x_1} f(Q_{22})\right) \\ &= \frac{1}{(x_2 - x_1)(y_2 - y_1)}(\\ &\quad f(Q_{11})(x_2 - x)(y_2 - y) + f(Q_{21})(x - x_1)(y_2 - y) \\ &\quad + f(Q_{12})(x_2 - x)(y - y_1) + f(Q_{22})(x - x_1)(y - y_1)\big) \\ &= \frac{1}{(x_2 - x_1)(y_2 - y_1)}\begin{bmatrix} x_2 - x & x - x_1 \end{bmatrix} \\ &\quad \cdot \begin{bmatrix} f(Q_{11}) & f(Q_{12}) \\ f(Q_{21}) & f(Q_{22}) \end{bmatrix} \begin{bmatrix} y_2 - y \\ y - y_1 \end{bmatrix} \end{aligned} \tag{3.17}$$

3.4 Conclution

Chapter 4

Deep Learning For Simulation

4.1 Convolutional Neural Networks

4.2 CNN Constructure

4.2.1 Convolutional layers

4.2.2 Full-connected layers

4.3 Traing configuration

4.3.1 Loss Function

4.3.2 Optimizer(SGD)

4.4 Training Results

4.5 Simulation based on Trained model

Chapter 5

Implementation

Chapter 6

Conclusion

6.1 Future work

References

[1] J. Tompson, K. Schlachter, P. Sprechmann, and K. Perlin, "Accelerating Eulerian Fluid Simulation With Convolutional Networks", *ArXiv e-prints*, Jul. 2016. arXiv: `1607.03597 [cs.CV]`.

[2] J. J. Monaghan, "Smoothed particle hydrodynamics", *Annual review of astronomy and astrophysics*, vol. 30, no. 1, pp. 543–574, 1992.

[3] M. Müller, D. Charypar, and M. Gross, "Particle-based fluid simulation for interactive applications", in *Proceedings of the 2003 ACM SIGGRAPH/Eurographics symposium on Computer animation*, Eurographics Association, 2003, pp. 154–159.

[4] M. Desbrun and M.-P. Gascuel, "Smoothed particles: A new paradigm for animating highly deformable bodies", in *Computer Animation and Simulation'96*, Springer, 1996, pp. 61–76.

[5] A. Paiva, F. Petronetto, T. Lewiner, and G. Tavares, "Particle-based non-newtonian fluid animation for melting objects", in *Computer Graphics and Image Processing, 2006. SIBGRAPI'06. 19th Brazilian Symposium on*, IEEE, 2006, pp. 78–85.